

Serum amyloid P colocalizes with apolipoproteins in human atheroma: functional implications[§]

Cameron R. Stewart,* Antonio Haw, III,[†] Roland Lopez,[†] Thomas O. McDonald,[†] Judy M. Callaghan,* Malcolm J. McConville,* Kathryn J. Moore,[§] Geoffrey J. Howlett,^{1,*} and Kevin D. O'Brien[†]

Department of Biochemistry and Molecular Biology,* Bio21 Molecular Science and Biotechnology Institute, University of Melbourne, Parkville, Victoria 3010, Australia; University of Washington Medical Center,[†] Seattle, WA 98195; and Lipid Metabolism Unit,[§] Massachusetts General Hospital, Harvard Medical School, Boston, MA 02114

Abstract Serum amyloid P (SAP) is a common component of human amyloid deposits and has been identified in atherosclerotic lesions. We investigated the extent of the colocalization of SAP with apolipoprotein A-I (apoA-I), apoB, apoC-II, and apoE in human coronary arteries and explored potential roles for SAP in these regions, specifically the effect of SAP on the rate of formation and macrophage recognition of amyloid fibrils composed of apoC-II. Analysis of 42 human arterial sections by immunohistochemistry and double label fluorescence microscopy demonstrated that SAP and apoA-I, apoB, apoC-II, and apoE were increased significantly in atherosclerotic lesions compared with nonatherosclerotic segments. SAP colocalized with all four apolipoproteins to a similar extent, whereas plaque macrophages were found to correlate most strongly with apoC-II and apoB. In vitro studies showed that SAP accelerated the formation of amyloid fibrils by purified apoC-II. Furthermore, SAP strongly inhibited the phagocytosis of apoC-II amyloid fibrils by primary macrophages and macrophage cell lines and blocked the resultant production of reactive oxygen species. **■** The ability of SAP to accelerate apoC-II amyloid fibril formation and inhibit macrophage recognition of apoC-II fibrils suggests that SAP may modulate the inflammatory response to amyloid fibrils in atherosclerosis.—Stewart, C. R., A. Haw, III, R. Lopez, T. O. McDonald, J. M. Callaghan, M. J. McConville, K. J. Moore, G. J. Howlett, and K. D. O'Brien. **Serum amyloid P colocalizes with apolipoproteins in human atheroma: functional implications.** *J. Lipid Res.* 2007. 48: 2162–2171.

Supplementary key words atherosclerosis • macrophage • immunohistochemistry • amyloid

Amyloid deposits are associated with several age-related diseases. Although intense research attention has focused on the deposits associated with neurodegeneration, particularly Alzheimer's and Parkinson's diseases, there is a

growing body of evidence that amyloid deposits are also associated with cardiovascular disease (1). Recent studies show that amyloid fibrils are present in up to 60% of aortic atherosclerotic lesions (2–4). Amyloid fibrils formed in the aortic media have been purified and the protein subunit identified as a 50 residue fragment of the cell surface protein lactadherin, termed medin (5). In contrast, a variety of different aggregates and amyloid-forming proteins have been identified in atherosclerotic lesions located in the intima. These proteins include serum amyloid A (SAA) (6), β -amyloid (A β) (1–42) (7, 8), transthyretin (9), α_1 -antitrypsin (10), and several plasma apolipoproteins, including apolipoprotein A-I (apoA-I), apoB, and apoE (2, 3, 11–15). The metabolic significance of these amyloid deposits is largely unknown.

Serum amyloid P (SAP) is a plasma glycoprotein that was first identified as a protein component of systemic amyloid deposits (16) and subsequently in cerebral amyloid deposits (17). SAP also localizes in a calcium-dependent manner within the intima of arterial atherosclerotic lesions at concentrations \sim 50 times higher than plasma SAP levels (18). The specificity of the interaction of SAP with amyloid fibrils is used clinically in whole body scintigraphy procedures, using labeled SAP to locate and monitor physiological amyloid deposits (19). The selective binding of SAP to amyloid fibrils in vivo raises the prospect that SAP may modulate the formation and metabolic fate of amyloid deposits in atherosclerotic lesions. SAP binds to amyloid fibrils formed by a diverse range of proteins, including A β (1–42) and A β (1–40) (20), SAA (21), β_2 -microglobulin (22), and apoC-II (23). Functional studies indicate that SAP inhibits

Abbreviations: A β , β -amyloid; AEDANS, ([amino]ethyl)amino-naphthalene-1-sulfonic acid; apoA-I, apolipoprotein A-I; DIT, diffuse intimal thickening; ROS, reactive oxygen species; SAA, serum amyloid A; SAP, serum amyloid P; ThT, thioflavin T.

¹ To whom correspondence should be addressed.

e-mail: ghowlett@unimelb.edu.au

§ The online version of this article (available at <http://www.jlr.org>) contains supplementary data in the form of five figures.

Manuscript received 23 February 2007 and in revised form 24 May 2007 and in re-revised form 3 July 2007.

Published, JLR Papers in Press, July 13, 2007.
DOI 10.1194/jlr.M700098-JLR200

the proteolytic degradation of A β , SAA, and systemic monoclonal light-chain amyloid fibrils (21) and promotes the self-association and tangling of apoC-II amyloid fibrils (23). SAP also binds to amyloid-like structures in oxidized LDL and inhibits the uptake of oxidized LDL by peritoneal macrophages (24).

Many of the proteins that form amyloid fibrils *in vivo* are members of the apolipoprotein family, including apoA-I, apoA-II, apoA-IV, and apoE, and the apolipoprotein-like proteins α -synuclein and SAA (25). *In vitro* studies of amyloid formation by apolipoproteins have focused on studies of human apoC-II. Under physiological conditions, apoC-II readily forms amyloid fibrils with a cross- β -sheet structure that reacts with the amyloid stains Congo Red and thioflavin T (ThT) (26). We have shown that apoC-II aggregates colocalize with SAP in atherosclerotic lesions (12). ApoC-II amyloid fibrils initiate macrophage inflammatory responses via the CD36 scavenger receptor, including increased reactive oxygen species (ROS) production and tumor necrosis factor- α expression (12). In a similar manner, fibrillar A β also initiates a CD36-mediated signaling cascade that stimulates the production of inflammatory mediators (27). This interaction with fibrillar A β competes with oxidized LDL for the CD36 receptor and reduces the accumulation of cholesterol derived from co-incubated oxidized LDL (28). These studies suggest that retained amyloid fibrils could modulate the inflammatory response and the activation of macrophage foam cells in atherosclerosis.

In this study, we extend our previous studies on the colocalization of apoC-II with SAP in atherosclerotic lesions (12) and consider the colocalization of SAP with other apolipoproteins. We also examine the *in vitro* effects of SAP on the formation and macrophage recognition of human apoC-II amyloid fibrils.

EXPERIMENTAL PROCEDURES

Human coronary arterial tissue

Human left anterior descending coronary segments ($n = 42$) were obtained from hearts removed from 20 patients at the time of cardiac transplantation. The coronary arteries were dissected free within 2 h of heart excision, fixed in 10% neutral buffered formalin, and embedded in paraffin. The use of human coronary artery tissue for these studies was approved by the University of Washington Human Subjects Review Committee. Using standard morphological criteria (29), these segments were classified as either atherosclerotic or diffuse intimal thickening (DIT). DIT represents the normal morphology of adult human coronary arteries (29), so the DIT segments represent nonatherosclerotic, control segments. Of the 42 segments, 33 were classified as atherosclerotic and 9 as DIT segments.

Immunohistochemistry

ApoE and apoA-I were detected using monospecific, goat polyclonal antiserum (30). ApoB was detected using a monospecific rabbit polyclonal antiserum (a kind gift from Dr. Thomas Innerarity, Gladstone Institute, San Francisco, CA) (31). SAP and apoC-II were detected using rabbit polyclonal antiserum

(Calbiochem, San Diego, CA). Single-label immunohistochemistry on single sections was performed as described previously (32, 33). Nova Red (Vector Laboratories, Burlingame, CA) was used as the peroxidase substrate, yielding a red-brown reaction product, and cell nuclei were counterstained with hematoxylin. Negative controls included omission of the primary antibody or antiserum as well as substitution of the primary antiserum with normal (nonimmune) rabbit or goat serum. Digital images of immunostained coronary artery sections were captured using a Nikon CoolPix 990 camera mounted on an Olympus BX50 microscope. Computer-assisted morphometry was performed using ImagePro Plus software (version 4.5.1; MediaCybernetics, Silver Spring, MD). Intimal areas were determined by manual tracing of boundaries of the intima, as represented by the arterial luminal border and the internal elastic lamina. Immunostained areas of HAM-56 (macrophages), SAP, apoA-I, apoB, apoC-II, and apoE were determined from digital images of their respective immunostained sections.

Double-label immunofluorescence

Tissue sections were deparaffinized and rehydrated through graded alcohols, incubated in 3% hydrogen peroxide for 10 min, washed in PBS, and incubated in antigen retrieval solution for 10 min (Target Retrieval Solution; DAKO Corp., Carpinteria, CA). The sections were washed in PBS and incubated with either anti-apoA-I (1:1,500) or anti-apoE (1:1,000) antiserum for 60 min. Samples were washed in PBS and incubated with a biotin-labeled anti-goat secondary antibody for 30 min and followed by a standard fluorophore, streptavidin Alexa Fluor[®] 488 conjugate (Molecular Probes-Invitrogen, Eugene, OR) for 30 min. Sections were washed with PBS and incubated with anti-SAP (1:100) antiserum for 60 min, then incubated with a standard fluorophore, Alexa Fluor[®] 555 goat anti-rabbit antibody (Molecular Probes-Invitrogen) for 30 min. Samples were washed and mounted with Vectashield Hard Set[™] mounting medium with 4',6-diaminophenylindole (Vector Laboratories). Samples were photographed as stacks using a Nikon Y-FL fluorescence microscope (Nikon, Melville, NY) at 40 \times magnification and a CoolSnapFX camera (Photometrics, San Diego, CA). The Z-axis progressions were done via a Z-Drive motor and controller, MFC-2000 (ASI, Eugene, OR). Photographs were taken using a Z-stepping of 0.2 μ m, 24 Z-steps from -2.4μ m to 2.4 μ m, with 0 μ m being the point of highest focus for each individual wavelength. The original images were deconvolved using the digital deconvolution module of MetaMorph (Molecular Devices, Sunnyvale, CA) using default settings and a 100 \times magnification bead stack as the reference source. The deconvolved images were overlaid to quantify colocalization. Quantification of colocalized areas was done using ImagePro Plus. Once areas were measured, the first and last six values were discarded and the rest of the areas were summed to obtain total areas of apoA-I, apoE, and SAP and colocalization of apoA-I with SAP and of apoE with SAP.

Protein purification and amyloid fibril preparation

ApoC-II was expressed and purified as described previously (26) and stored as a concentrated stock in 5 M GuHCl. SAP was purified from human plasma (23) and stored at -20° C in 20 mM Tris-HCl and 140 mM NaCl, pH 7.4. ApoC-II amyloid fibrils were prepared by direct dilution (1:100) of a concentrated stock solution of apoC-II in 5 M GuHCl into refolding buffer (20 mM Tris-HCl, 140 mM NaCl, and 1 g/l sodium azide, pH 7.4). For cell culture, proteins were dialyzed against 20 mM Tris-HCl and 140 mM NaCl, pH 7.4, to remove residual azide and other salts. ([Amino]ethyl)amino-naphthalene-1-sulfonic acid (AEDANS)-labeled apoC-II was provided by Emma Lees and Chi Pham

(University of Melbourne) and prepared by chemical modification of a cysteine-containing derivative of apoC-II with 5-((2-iodoacetyl)amino)ethyl]amino)-naphthalene-1-sulfonic acid using procedures similar to those described previously (34). Micromolar concentrations of SAP and apoC-II monomer or fibrils are expressed on the basis of the molecular weights of the SAP pentamer and monomeric apoC-II, respectively.

ThT fluorescence assays

ApoC-II and SAP were diluted from stock solutions into refolding buffer and incubated at room temperature without stirring. At specified time points, 25 μ l sample aliquots were added to the wells of a microtiter plate containing refolding buffer and 8 μ M ThT to a final volume of 250 μ l. Fluorescence intensities were measured using a f_{\max} fluorescence plate reader (Molecular Devices) with an 444 nm/485 nm excitation/emission filter set. The half-time for amyloid fibril formation was calculated as described previously (35).

Sedimentation velocity analysis

Sedimentation velocity analysis was performed using a Beckman model XL-A analytical ultracentrifuge at 20°C as described previously (24). SAP was centrifuged at 25,000 rpm with radial absorbance data acquired at 230 nm and radial increments of 0.002 cm in the continuous scanning mode. Radial scans were taken at 10 min intervals. Data were fitted to a continuous size distribution model using SEDFIT software (36).

Macrophages

The murine macrophage cell line J774.1 was maintained as a monolayer in 25 cm² flasks at 37°C and 5% CO₂ in RPMI medium supplemented with 10% heat-inactivated fetal bovine serum, 100 U/ml penicillin, and 100 μ g/ml streptomycin. Elicited peritoneal macrophages were collected from mice by peritoneal lavage at 4 days after intraperitoneal injection with 3% thioglycolate as described previously (27) and cultured in DMEM containing 2% fetal bovine serum, 100 U/ml penicillin, and 100 μ g/ml streptomycin overnight at 37°C before use. All animal procedures were approved by the Massachusetts General Hospital Subcommittee on Research Animal Care and were conducted in accordance with the U. S. Department of Agriculture Animal Welfare Act for the Humane Care and Use of Laboratory Animals.

ROS production

ROS production was measured by nitroblue tetrazolium reduction assay (12). J774.1 macrophages (2×10^5) were incubated on 6 mm² multispot slides in DMEM (500 μ l) containing fetal bovine serum for 1 h and stimulated with apoC-II fibrils (6.73 μ M) in the absence and presence of SAP (0.15 μ M) and calcium (2 mM) for 10 min at 37°C. ROS production was measured by absorbance spectroscopy at 650 nm. For experiments using peritoneal macrophages, macrophages (2×10^5) were incubated with apoC-II (20 μ M) and SAP (0.8–2.35 μ M) in the presence of 2 mM calcium. ROS production was quantified by microscope video capture (five measurements per sample) with ImageQuant analysis software.

Macrophage uptake of fluorescently labeled apoC-II fibrils

J774.1 murine macrophages were seeded at a concentration of 2×10^5 cells/500 μ l on a 24-well plate and incubated overnight at 37°C and 5% CO₂. Cells were incubated with AEDANS-labeled apoC-II fibrils (6.73 μ M) in the presence or absence of SAP

(0.15 μ M) and 2 mM CaCl₂. Samples without calcium contained 0.5 mM EDTA. Samples were incubated for 5, 24, and 48 h at 37°C and 5% CO₂. The unbound fibrils were removed by repeated washing with warm serum-free RPMI, and samples were resuspended in 500 μ l of 5 M GuHCl and 10 mM Tris-HCl, pH 8.0. Fluorescence emission spectra were obtained using a SPEX Fluorolog/Tau-2 spectrofluorometer and a 5 mm path length cuvette. Excitation/emission wavelength settings were 336 and 490 nm, respectively, with excitation and emission slit widths of 2 nm. Cellular protein content was measured by BCA assay (Pierce, Rockford, IL). All measurements were performed in triplicate. Cell-associated fluorescence increased systematically over the first 24 h, with a subsequent decline after 48 h. Results are reported for cells incubated for 24 h.

Peritoneal macrophages (2×10^5) on 48-well plates were cooled to 4°C for 20 min, 5.6 μ M fibrils were added for 30 min at 4°C, and then cells were incubated at 37°C for 30 min to allow internalization. Cells were placed on ice to stop internalization and were maintained on ice for the remainder of the assay. Total cell-associated fluorescence was measured by flow cytometry (5,000 events) using the CellQuest program (Becton Dickinson). Fibril internalization was measured by quenching extracellular fluorescence with 0.2% trypan blue immediately before analysis. The phagocytosis index was expressed as the percentage of fluorescence-positive cells multiplied by the mean fluorescence of these cells. All treatments were performed in triplicate, and data are presented as means \pm SD.

Fluorescence microscopy

J774.1 macrophages were grown on 10 mm coverslips before the addition of AEDANS-labeled apoC-II fibrils. Coverslips were incubated for 24 h at 37°C and 5% CO₂, and the unbound fibrils were removed by repeated washing with warm serum-free RPMI followed by PBS. The macrophages were fixed with methanol for 10 min. After washing three times with PBS, the coverslips were mounted with Mowiol mounting medium and viewed using a Zeiss Axioplan2 microscope and an AxioCam MRm digital camera.

RESULTS

Coronary artery segments classified as atherosclerotic ($n = 33$) or DIT ($n = 9$) were immunostained with specific antiserum. Typical results are shown in **Figs. 1A–D** for SAP, apoA-I, and apoE, where the extensive red staining shows that these antigens are present within the atherosclerotic arterial intima. There was no positive immunostaining in adjacent sections in which either normal rabbit serum or normal goat serum was substituted for the primary antiserum. Immunostaining of a control DIT section (see supplementary Fig. 1) showed only faint SAP staining along the internal elastic lamina of the artery section, with no visible apoA-I staining. This weak staining is consistent with reports that limited amounts of SAP are found in association with elastic fibers in normal arteries (37). A comparison of immunostaining for SAP and apoE in a normal DIT segment and in a plaque segment is presented in supplementary Fig. II. In the DIT segment (upper panels), there is very little staining above background for either SAP or apoE, whereas in the plaque segment (lower panels), there is widespread staining for both SAP and apoE.

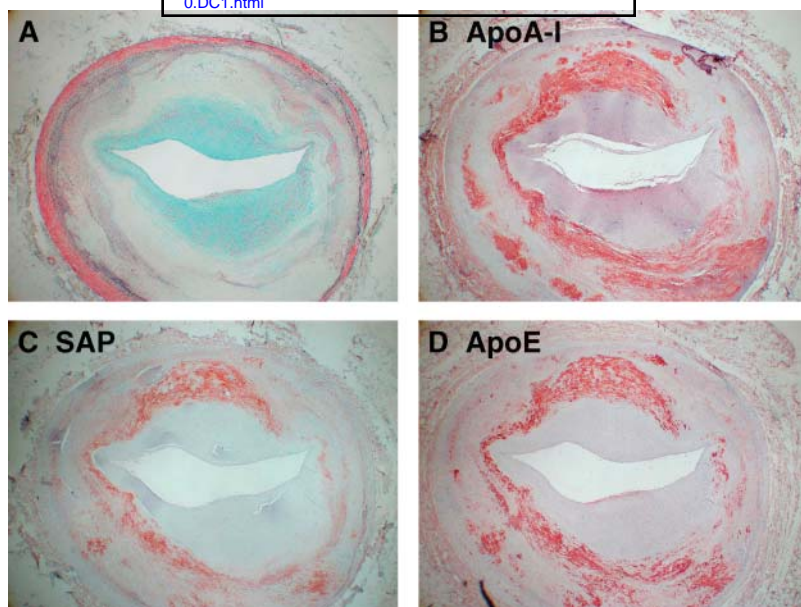


Fig. 1. Adjacent sections of a human atherosclerotic plaque stained with the Movat's pentachrome stain (A) or with monospecific antiserum to apolipoprotein A-I (apoA-I) (B), serum amyloid P (SAP) (C), or apoE (D). For Movat's stain, cells are red, elastin is black, collagen is yellow, and glycosaminoglycans are blue. Positive immunostaining is identified by a red-brown reaction product. Original magnification, 40 \times .

Arterial sections were also immunostained for apoB, apoC-II, and HAM56, a specific antibody for macrophages. The photomicrographs in **Fig. 2** show significant SAP, apoC-II, and apoB immunoreactivity associated with the atherosclerotic arterial intima (**Fig. 2**). The Movat's stain in **Fig. 2A** shows grayish-black staining that is indicative of elastin fibers. SAP localization in **Fig. 2B** is in the same region as some elastin fibers but is broader and appears to be colocalized with areas of blue staining, indicating glycosaminoglycans adjacent to these elastin fibers (see supplementary **Fig. III**). Analysis of 32 atherosclerotic plaque sections and 9 control DIT sections demonstrated significant immunoreactivity for SAP, apoA-I, and apoE in all but one of the atherosclerotic lesions tested, with less frequent presence in DIT sections (**Table 1**). Immunoreactivity for apoC-II and apoB was observed in a lower proportion of atherosclerotic lesions compared with apoA-I and apoE but was present at higher frequency compared with apoB and apoC-II in DIT sections.

We used quantitative immunohistochemistry of the 32 plaque sections to determine the SAP- and macrophage-containing areas and the areas containing specific apolipoproteins. The SAP areas in atherosclerotic lesions correlated significantly with the areas determined for apoE and apoA-I (**Table 2**). The lack of correlation between plaque SAP and apoB and apoC-II (**Table 2**) can be attributed to the observation that SAP was present in 32 of 33 plaques, whereas apoB and apoC-II were detected in only 16 of 33 and 12 of 33 sections, respectively. In contrast, the plaque macrophage area correlated most strongly with the areas determined for apoC-II, followed by the area for apoB (**Table 3**). There was no significant correlation of macrophage area with the areas determined for either apoA-I or apoE.

The arterial sections described in **Table 1** were examined in greater detail to determine the colocalization of SAP with apolipoproteins. Each of the 42 coronary segments was scored for the presence or absence of colocalization, as determined by side-by-side comparison of the immunostained sections. An example of the computer-assisted morphometry approach taken is shown in supplementary **Fig. IV**. The positive immunostained area for SAP was captured and assigned the color green (see supplementary **Fig. IVB**). Similarly, the positive immunostained area for apoE was captured and assigned a dark blue color. If the light blue (cyan) color appeared when the images merged, then colocalization was scored as present for that coronary artery segment. Colocalized areas for SAP and each of the individual apolipoproteins were determined by merging pseudocolor images of immunostained areas obtained from adjacent sections. Colocalization of SAP with apoA-I and apoE was detected in the majority of atherosclerotic plaques tested but in fewer control (DIT) segments (**Table 4**). Similarly, colocalization of SAP with apoB and apoC-II was detected in a much higher proportion of plaque sections compared with DIT sections. Overall, SAP colocalized with apoA-I, apoB, apoC-II, and apoE in 32 of 33 of plaque sections but in only 2 of 9 DIT sections. This difference in prevalence was highly significant ($P < 0.0001$ by Fisher's exact test) and suggests that SAP colocalization with retained apolipoproteins is a characteristic of coronary atherosclerotic plaques.

We next sought to determine whether SAP colocalized preferentially with apoA-I, apoB, apoC-II, and apoE in atherosclerotic plaque segments. Sections stained for specific apolipoproteins were analyzed for the extent of colocalization with SAP in adjacent sections. In experiments in which immunostaining was performed for a single antigen

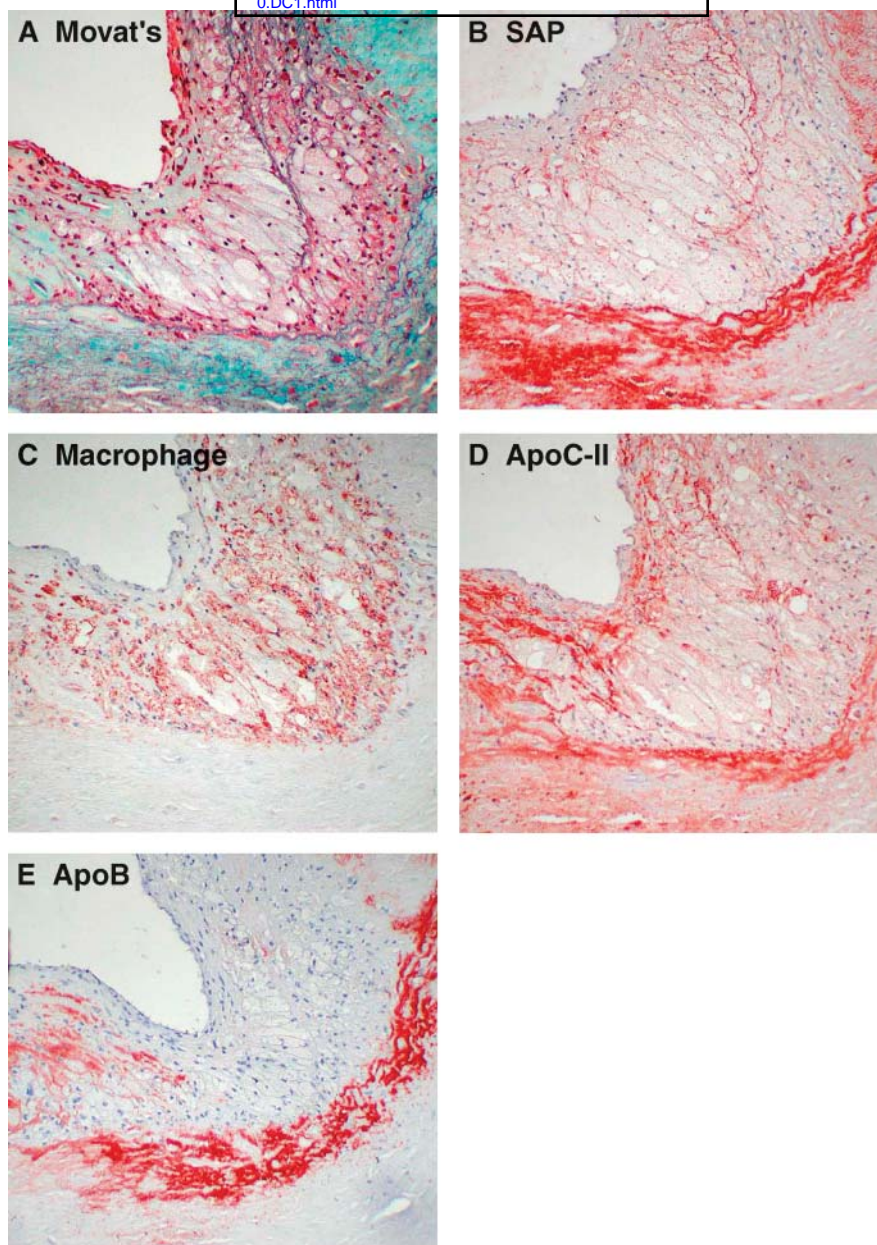


Fig. 2. Adjacent sections of an atherosclerotic plaque stained with Movat's histochemical stain (A) or immunostained for SAP (B), macrophages (C), apoC-II (D), or apoB (E). Original magnification, 200 \times .

(apoA-I) on consecutive histological sections from nine different human coronary atherosclerotic segments, the colocalization for this method was $80.9 \pm 6.6\%$ for exactly adjacent sections and $65.3 \pm 18.5\%$ for sections separated by one intervening section. Therefore, this method likely underestimates the extent of colocalization of different antigens. The proportion of each apolipoprotein that colocalized with SAP in plaque tissue is shown in **Fig. 3A**. SAP colocalized to an equal extent with apoA-I, apoB, apoC-II, and apoE, with an average of $\sim 20\%$ of the apolipoprotein staining colocalized with SAP.

Colocalization studies that compare the staining of adjacent single-label sections are limited by the assumption that sections are not distorted during preparation and that

the distribution of immunoreactivities is identical in adjacent sections. To overcome these limitations and to obtain independent confirmation of the results presented in **Fig. 3A**, we examined the colocalization of SAP with apoA-I and apoE within single arterial sections using double-label fluorescence microscopy. **Figure 3B, C** shows that the percentages of apoA-I and apoE that colocalized with SAP were increased significantly in atherosclerotic tissue compared with DIT sections ($P < 0.05$ by two-tailed Student's *t*-test). The results for the colocalization of apoA-I with SAP using double-label fluorescence microscopy were similar to the results obtained using immunohistochemistry of adjacent sections, whereas the degree of colocalization of apoE with SAP was slightly higher using the double-label

TABLE 1. Proportion of plaque and DIT arterial sections positive for SAP and apoA-I, apoB, apoC-II, and apoE

Positive Localization	Plaque (n = 33)	DIT (n = 9)
	<i>n</i> (%)	
SAP	32 (97)	5 (56)
Macrophages	12 (36)	0 (0)
ApoA-I	32 (97)	2 (22)
ApoE	32 (97)	2 (22)
ApoB	17 (52)	1 (11)
ApoC-II	13 (39)	2 (22)

ApoA-I, apolipoprotein A-I; DIT, diffuse intimal thickening; SAP, serum amyloid P.

approach. The absolute values obtained for colocalization using the double-label approach depend on the sensitivity of the detecting antibodies. The important observation remains that quantitative immunostaining using both single- and double-label immunohistochemistry showed that colocalization of SAP with apolipoproteins is increased significantly in atherosclerotic lesions compared with control DIT sections. This raises the prospect that SAP may fulfill important functional roles within atherosclerotic lesions.

We examined the effect of SAP on amyloid fibril formation by human apoC-II. Initial experiments were designed to characterize the solution behavior of SAP in the presence and absence of calcium. Sedimentation velocity analysis of SAP in the absence of calcium yielded a skewed sedimentation coefficient distribution, with an average sedimentation coefficient of 9 S (see supplementary Fig. V), consistent with previous studies showing that SAP in the absence of calcium exists primarily as a decamer (38). The skewed shape of the distribution curve indicates the presence of slower sedimenting species attributed to the presence of a small amount of pentamer in equilibrium with the decamer. The sedimentation coefficient of SAP in the presence of 1 mM calcium indicated a homogeneous pentamer with a sedimentation coefficient of 6.9 S. Sedimentation velocity analysis of SAP in the presence of 2 mM calcium revealed small amounts of aggregated protein (data not shown), consistent with reports of SAP aggregation in the presence of higher calcium concentrations (39).

To assess the effect of SAP on amyloid formation by apoC-II, we incubated the amyloid-reactive dye ThT with mixtures of apoC-II and SAP in the presence and absence of 1 mM calcium. Amyloid fibril formation by apoC-II (42 μ M) showed an initial lag phase of \sim 6 h, followed by a steady increase in ThT fluorescence, corresponding to

TABLE 2. Correlations of SAP area with apolipoprotein areas in 32 human coronary atherosclerotic plaques

Apolipoprotein	<i>r</i>	<i>P</i>
ApoE	0.64	<0.0001
ApoA-I	0.47	0.006
ApoB	0.15	0.43
ApoC-II	0.14	0.44

TABLE 3. Correlations of macrophage area with apolipoprotein areas in 32 human coronary atherosclerotic plaques

Apolipoprotein	<i>r</i>	<i>P</i>
ApoC-II	0.52	0.0031
ApoB	0.41	0.0282
ApoA-I	0.29	0.12
ApoE	0.21	0.27

the formation of amyloid fibrils (Fig. 4). The addition of calcium (1 mM) and substoichiometric concentrations of SAP (780 nM pentamer) caused an immediate increase in ThT fluorescence, with a reduction in the half-time for fibril formation from 16 to 5 h. Significant acceleration of apoC-II fibril formation was also observed at lower concentrations of SAP (196 and 392 nM). Control experiments showed that calcium alone did not influence the ThT fluorescence profile of apoC-II fibrillogenesis. ApoC-II fibril formation was not affected by SAP in the absence of calcium, and SAP alone did not contribute to ThT fluorescence levels. Incubating apoC-II with the related pentraxin C-reactive protein at concentrations of 100 nM, 1 μ M, and 2 μ M, both in the absence and in the presence of 1 mM calcium, had no significant effect on the formation of apoC-II amyloid fibrils (data not shown).

We next investigated whether SAP affected macrophage activation by fibrillar apoC-II by measuring the production of ROS using the murine macrophage cell line J774.1. Fibrillar apoC-II induced ROS generation by macrophages, and this inflammatory response was inhibited significantly by SAP in a calcium-dependent manner (Fig. 5A). SAP or calcium alone did not contribute to ROS levels, indicating that SAP specifically reduces the macrophage reactive oxygen response to amyloid. We extended this investigation by determining the effect of SAP on the uptake and internalization of fluorescence-labeled apoC-II fibrils by these cells (Fig. 5B). The uptake of AEDANS-labeled apoC-II fibrils measured by fluorescence spectroscopy, expressed per microgram of total protein in the macrophage extract, was reduced to 59% of the control value by SAP in the presence of calcium (2 mM), while in the absence of calcium, SAP had no effect on the process. Confirmation of the effect of SAP on the uptake of AEDANS-labeled apoC-II fibrils was provided by fluorescence microscopy (Fig. 5C). The extensive fluorescence associated with the uptake of AEDANS-labeled apoC-II fibrils by macrophages was reduced significantly by SAP in a calcium-dependent manner.

The effect of SAP on the activation of macrophages by apoC-II fibrils was confirmed in primary peritoneal mac-

TABLE 4. Number of plaque and DIT arterial sections positive for the colocalization of SAP with apoA-I, apoB, apoC-II, and apoE

Apolipoprotein	Plaque (n = 33)	DIT (n = 9)
	<i>n</i> (%)	
ApoA-I	32 (97)	2 (22)
ApoE	32 (97)	2 (22)
ApoB	16 (48)	1 (11)
ApoC-II	12 (36)	2 (22)

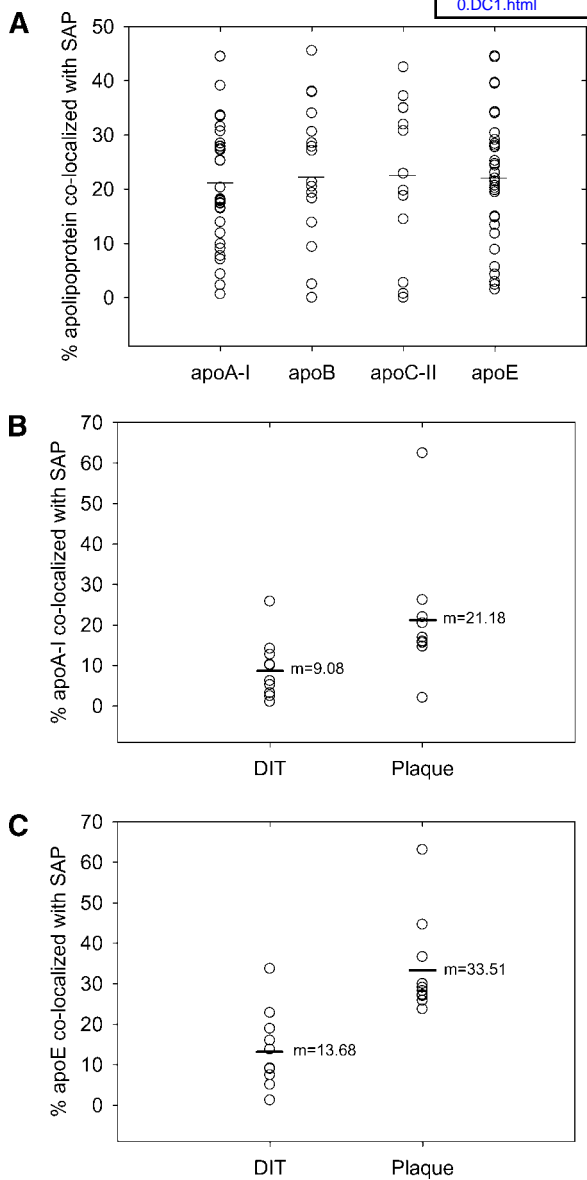


Fig. 3. A: Single-label immunostaining of sequential arterial sections was used to measure the percentage of apoA-I, apoB, apoC-II, and apoE that colocalized with SAP within atherosclerotic lesions. B, C: Double-label immunostaining was used to measure the percentage of apoA-I (B) and apoE (C) that colocalized with SAP in atherosclerotic and diffuse intimal thickening (DIT) sections. The mean values in A are 21.10, 22.14, 22.44, and 21.97 for apoA-I, apoB, apoC-II, and apoE, respectively. The mean values (m) in B and C are indicated.

rophages (**Fig. 6**). SAP binding to apoC-II fibrils strongly inhibited peritoneal macrophage ROS production in a concentration-dependent manner, whereas BSA had no effect at comparable concentrations. We used analytical flow cytometry to examine the effect of SAP on apoC-II fibril phagocytosis in peritoneal macrophages (**Fig. 6B**). SAP inhibited the uptake of fluorescently labeled apoC-II fibrils (5.6 μ M), with significant inhibition observed at both low (39 nM) and high (395 nM) SAP concentrations. These results show that SAP inhibits the activation of

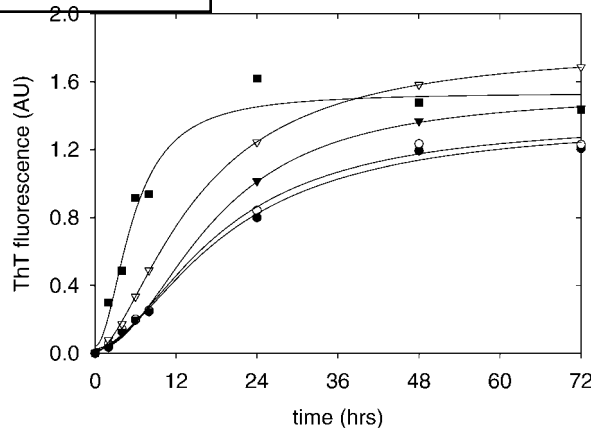


Fig. 4. Thioflavin T (ThT) fluorescence assay of apoC-II (42 μ M) incubated alone (closed circles) or with SAP (780 nM) and 0 mM calcium (open circles). ApoC-II (42 μ M) was also incubated with increasing concentrations of SAP and 1 mM CaCl₂. The concentrations of SAP are 190 nM (closed triangles), 390 nM (open triangles), and 780 nM (closed squares). AU, arbitrary units.

macrophages by apoC-II amyloid fibrils and inhibits the phagocytosis of apoC-II fibrils.

DISCUSSION

We have demonstrated that SAP colocalizes with retained apoA-I, apoB, apoC-II, and apoE at significantly higher levels in human atheroma than in control DIT sections. Although SAP was detected to an equal extent with all four apolipoproteins examined, SAP deposition correlated most strongly with apoA-I and apoE. The lack of any significant correlation of apoC-II or apoB deposition with SAP deposition was attributed to the observation that not all atherosclerotic lesions contained apoC-II and apoB. Conversely, a strong correlation existed between apoC-II and macrophage deposition. In addition to plasma lipoproteins, macrophages are a potent source of apoC-II in plaques, as apoC-II secretion is upregulated in macrophage foam cells (40). If activated macrophages are the major source of apoC-II fibrils present in atheroma, one would expect a poor correlation between SAP and apoC-II in chronic, stable atherosclerotic plaques containing very few macrophages. This does not exclude a potentially important role for SAP in apoC-II fibrillogenesis in the local environment surrounding macrophages of unstable, macrophage-rich plaques.

The use of labeled SAP in scintigraphy studies provides a *prima facie* case for the presence of amyloid fibrils in tissues (12). It is therefore of interest to consider whether the colocalization of SAP with apolipoproteins in atherosclerotic tissue indicates the presence of aggregated apolipoproteins with amyloid-like properties. In the case of apoB, the principal protein component of LDL, our previous studies show that SAP binds to oxidized forms of LDL, but not native LDL (24). Thus, the colocalization of SAP with apoB may indicate the presence of oxidized

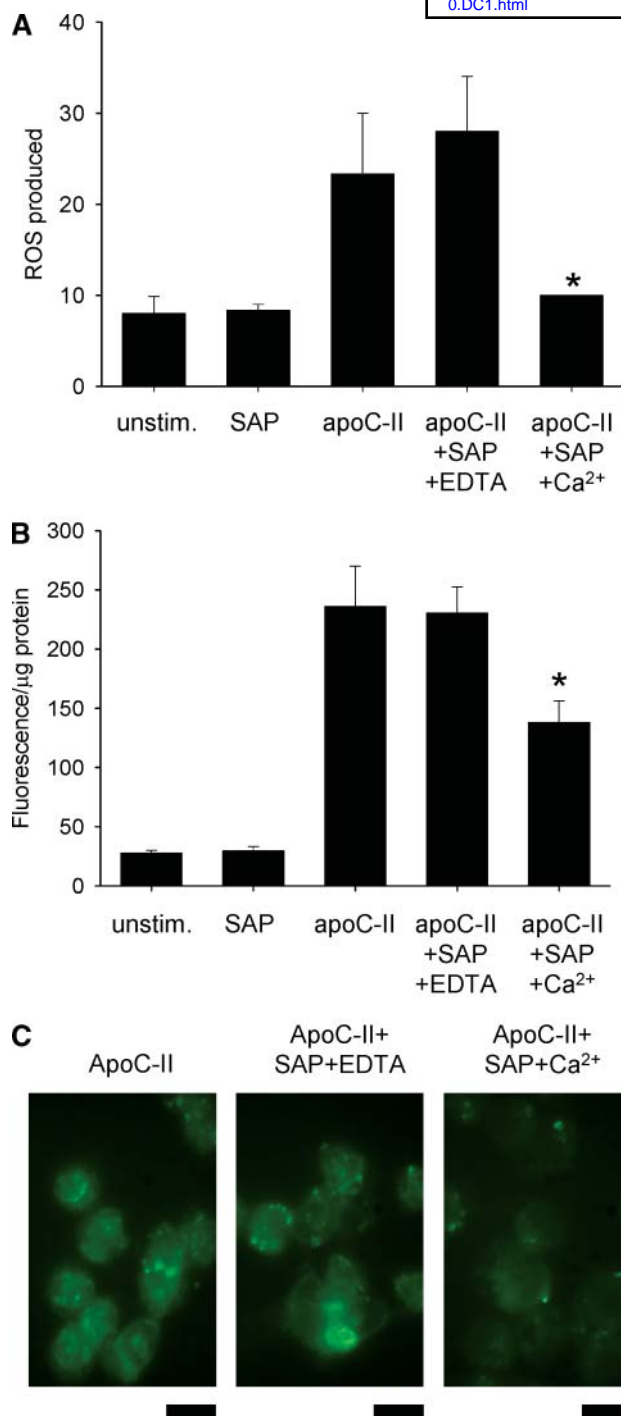


Fig. 5. A: Reactive oxygen species (ROS) generated by J774.1 macrophages incubated with apoC-II fibrils. Error bars represent SD. * $P < 0.05$, significantly different from macrophages incubated with apoC-II fibrils alone, by two-tailed Student's *t*-test. B: Uptake and internalization of fluorescently labeled apoC-II fibrils by J774.1 macrophages. The fluorescence was measured by spectrophotometry on triplicate samples. Data presented are representative of three separate experiments. Error bars represent SD. * $P < 0.05$, significantly different from macrophages incubated with apoC-II fibrils alone, by two-tailed Student's *t*-test. C: Immunofluorescence microscopy of J774.1 macrophages incubated with ([amino]ethyl)amino-naphthalene-1-sulfonic acid-labeled apoC-II fibrils (6.73 μM) in the presence or absence of SAP (0.15 μM) and 2 mM CaCl₂. Bars = 10 μM.

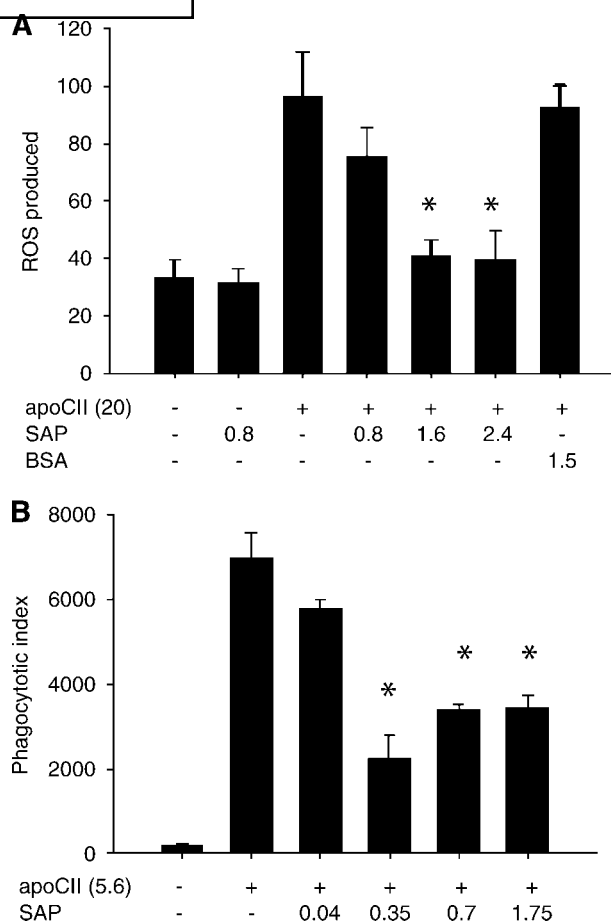



Fig. 6. A: Production of ROS by peritoneal macrophages in response to apoC-II fibrils, calcium, and SAP. Points represent means of triplicate samples. Error bars represent SD. * $P < 0.05$, significantly different from macrophages incubated with apoC-II fibrils alone, by two-tailed Student's *t*-test. B: Phagocytosis of fluorescently labeled apoC-II fibrils was quantified by fluorescence-assisted flow cytometry. Error bars represent SD. * $P < 0.05$, significantly different from macrophages incubated with apoC-II fibrils alone, by two-tailed Student's *t*-test.

LDL, consistent with studies that have identified oxidized LDL in atherosclerotic plaques (41). Recent studies have shown that apoE forms fibrils in vitro with properties of amyloid (42). However, apoE is also considered a universal component of amyloid deposits, able to bind to diverse amyloid fibrils, including apoC-II fibrils (23). Thus, the colocalization of apoE with SAP may simply indicate the general ability of apoE and SAP to interact with amyloid fibrils. Familial cases of apoA-I systemic amyloidosis establish the capacity of apoA-I and its truncated derivatives to form amyloid fibrils in vivo (2, 3). One explanation for the colocalization of SAP with apoA-I in atherosclerotic sections is that SAP interacts specifically with deposits of apoA-I fibrils. Alternatively, our recent studies have identified HDL as a major amyloid fibril binding species in plasma (43), capable of interacting with both apoC-II and Aβ amyloid fibrils. Thus, the colocalization of apoA-I, a major protein component of HDL, with SAP may signal the retention of HDL particles in atherosclerotic plaques

arising from a specific interaction with amyloid fibrils. ApoC-II amyloid fibrils form readily in vitro and interact specifically with SAP (23). Therefore, the colocalization of SAP with apoC-II in atherosclerotic plaques provides indirect evidence for the presence of apoC-II fibrils in vivo. The use of Congo Red birefringence to detect amyloid deposits in atherosclerotic plaques does not allow the identification of the specific fibrillar proteins that interact with Congo Red. Direct evidence for specific proteins as fibrillar amyloid components in atherosclerotic plaques requires the future development of reagents that can distinguish fibrillar and nonfibrillar forms of the protein.

SAP plasma levels correlate with several cardiovascular disease risk factors, including myocardial infarction and angina (44). Therefore, it is relevant to discuss how the functions of SAP described in this study may influence atherosclerosis. A potentially proatherogenic effect is that SAP accelerates amyloid fibril formation and inhibits phagocytotic degradation in a manner that may contribute to the ongoing accumulation and persistence of amyloid deposits. Mature apoC-II and A β amyloid fibrils both initiate proinflammatory signaling cascades that would be expected to exacerbate inflammation in atherosclerosis (12, 27). The inhibitory effect of SAP on the phagocytosis of apoC-II amyloid fibrils is consistent with the antiopson properties of SAP (45). A role for SAP as a regulator of amyloid fibril deposition is consistent with the observation that amyloid deposits form more slowly in mice lacking SAP than in wild-type mice when amyloid A amyloidosis is induced in response to chronic inflammation (46). Offsetting these potentially proatherogenic effects of SAP are studies showing that for many amyloid systems, oligomeric species formed during the early stages of amyloid fibril formation are cytotoxic (47). A functional role for SAP in atherosclerosis may be to convert cytotoxic oligomeric species into less toxic mature amyloid fibrils. Our work suggests that SAP limits the macrophage production of reactive oxygen in response to amyloid. Thus, the binding of SAP to fibrillar apolipoproteins in areas of colocalization within atheroma may prevent fibril recognition by macrophage scavenger receptors, thus reducing the inflammatory potential. Further studies of the ramifications of SAP colocalization with apolipoproteins in atheroma may resolve some of these apparently conflicting roles for SAP in disease development and shed light on the link between plasma SAP levels and the risk of cardiovascular disease (44). 

This work was supported by Grant 350229 from the National Health and Medical Research Council to G.J.H.

REFERENCES

1. Howlett, G. J., and K. J. Moore. 2006. Untangling the role of amyloid in atherosclerosis. *Curr. Opin. Lipidol.* **17**: 541–547.
2. Mucchiano, G. I., L. Jonasson, B. Haggqvist, E. Einarsson, and P. Westermark. 2001. Apolipoprotein A-I-derived amyloid in atherosclerosis. Its association with plasma levels of apolipoprotein A-I and cholesterol. *Am. J. Clin. Pathol.* **115**: 298–303.

3. Mucchiano, G. I., B. Haggqvist, K. Sletten, and P. Westermark. 2001. Apolipoprotein A-I-derived amyloid in atherosclerotic plaques of the human aorta. *J. Pathol.* **193**: 270–275.
4. Rocken, C., J. Tautenhahn, F. Buhling, D. Sachwitz, S. Vockler, A. Goette, and T. Burger. 2006. Prevalence and pathology of amyloid in atherosclerotic arteries. *Arterioscler. Thromb. Vasc. Biol.* **26**: 676–677.
5. Haggqvist, B., J. Naslund, K. Sletten, G. T. Westermark, G. Mucchiano, L. O. Tjernberg, C. Nordstedt, U. Engstrom, and P. Westermark. 1999. Medin: an integral fragment of aortic smooth muscle cell-produced lactadherin forms the most common human amyloid. *Proc. Natl. Acad. Sci. USA.* **96**: 8669–8674.
6. O'Brien, K. D., T. O. McDonald, V. Kunjathoor, K. Eng, E. A. Knopp, K. Lewis, R. Lopez, E. A. Kirk, A. Chait, T. N. Wight, et al. 2005. Serum amyloid A and lipoprotein retention in murine models of atherosclerosis. *Arterioscler. Thromb. Vasc. Biol.* **25**: 785–790.
7. Koldamova, R., M. Staufenbiel, and I. Lefterov. 2005. Lack of ABCA1 considerably decreases brain apoE level and increases amyloid deposition in APP23 mice. *J. Biol. Chem.* **280**: 43224–43235.
8. Hirsch-Reinshagen, V., L. F. Maia, B. L. Burgess, J. F. Blain, K. E. Naus, S. A. McIsaac, P. F. Parkinson, J. Y. Chan, G. H. Tansley, M. R. Hayden, et al. 2005. The absence of ABCA1 decreases soluble apoE levels but does not diminish amyloid deposition in two murine models of Alzheimer disease. *J. Biol. Chem.* **280**: 43243–43256.
9. Jacobson, D. R., M. Ittmann, J. N. Buxbaum, R. Wiczorek, and P. D. Gorevic. 1997. Transthyretin Ile 122 and cardiac amyloidosis in African-Americans. Two case reports. *Tex. Heart Inst. J.* **24**: 45–52.
10. Janciauskiene, S., P. Garcia de Frutos, E. Carlemalm, B. Dahlback, and S. Eriksson. 1995. Inhibition of Alzheimer beta-peptide fibril formation by serum amyloid P component. *J. Biol. Chem.* **270**: 26041–26044.
11. Westermark, P., G. Mucchiano, T. Marthin, K. H. Johnson, and K. Sletten. 1995. Apolipoprotein A1-derived amyloid in human aortic atherosclerotic plaques. *Am. J. Pathol.* **147**: 1186–1192.
12. Medeiros, L. A., T. Khan, J. B. El Khoury, C. L. Pham, D. M. Hatters, G. J. Howlett, R. Lopez, K. D. O'Brien, and K. J. Moore. 2004. Fibrillar amyloid protein present in atheroma activates CD36 signal transduction. *J. Biol. Chem.* **279**: 10643–10648.
13. Rosenfeld, M. E., S. Butler, V. A. Ord, B. A. Lipton, C. A. Dyer, L. K. Curtiss, W. Palinski, and J. L. Witztum. 1993. Abundant expression of apoprotein E by macrophages in human and rabbit atherosclerotic lesions. *Arterioscler. Thromb.* **13**: 1382–1389.
14. O'Brien, K. D., S. S. Deeb, M. Ferguson, T. O. McDonald, M. D. Allen, C. E. Alpers, and A. Chait. 1994. Apolipoprotein E localization in human coronary atherosclerotic plaques by in situ hybridization and immunohistochemistry and comparison with lipoprotein lipase. *Am. J. Pathol.* **144**: 538–548.
15. Bedossa, P., T. Poynard, A. Abella, F. Paraf, G. Lemaigre, and E. Martin. 1989. Localization of apolipoprotein A-I and apolipoprotein A-II in human atherosclerotic arteries. *Arch. Pathol. Lab. Med.* **113**: 777–780.
16. Cathcart, E. S., F. A. Wollheim, and A. S. Cohen. 1967. Plasma protein constituents of amyloid fibrils. *J. Immunol.* **99**: 376–385.
17. Coria, F., E. Castano, F. Prelli, M. Larrondo-Lillo, S. van Duinen, M. L. Shelanski, and B. Frangione. 1988. Isolation and characterization of amyloid P component from Alzheimer's disease and other types of cerebral amyloidosis. *Lab. Invest.* **58**: 454–458.
18. Li, X. A., K. Hatanaka, H. Ishibashi-Ueda, C. Yutani, and A. Yamamoto. 1995. Characterization of serum amyloid P component from human aortic atherosclerotic lesions. *Arterioscler. Thromb. Vasc. Biol.* **15**: 252–257.
19. Hawkins, P. N., M. J. Myers, J. P. Lavender, and M. B. Pepys. 1988. Diagnostic radionuclide imaging of amyloid: biological targeting by circulating human serum amyloid P component. *Lancet.* **1**: 1413–1418.
20. Hamazaki, H. 1995. Ca(2+)-dependent binding of human serum amyloid P component to Alzheimer's beta-amyloid peptide. *J. Biol. Chem.* **270**: 10392–10394.
21. Tennent, G. A., L. B. Lovat, and M. B. Pepys. 1995. Serum amyloid P component prevents proteolysis of the amyloid fibrils of Alzheimer disease and systemic amyloidosis. *Proc. Natl. Acad. Sci. USA.* **92**: 4299–4303.
22. Myers, S. L., S. Jones, T. R. Jahn, I. J. Morten, G. A. Tennent, E. W. Hewitt, and S. E. Radford. 2006. A systematic study of the effect of physiological factors on beta2-microglobulin amyloid formation at neutral pH. *Biochemistry.* **45**: 2311–2321.

23. MacRaidl, C. A., C. R. Stewart, Y. F. Mok, M. J. Gunzburg, M. A. Perugini, L. J. Lawrence, V. Tirtaatmadja, J. J. Cooper-White, and G. J. Howlett. 2004. Non-fibrillar components of amyloid deposits mediate the self-association and tangling of amyloid fibrils. *J. Biol. Chem.* **279**: 21038–21045.
24. Stewart, C. R., A. A. Tseng, Y. F. Mok, M. K. Staples, C. H. Schiesser, L. J. Lawrence, J. N. Varghese, K. J. Moore, and G. J. Howlett. 2005. Oxidation of low-density lipoproteins induces amyloid-like structures that are recognized by macrophages. *Biochemistry.* **44**: 9108–9116.
25. Hatters, D. M., and G. J. Howlett. 2002. The structural basis for amyloid formation by plasma apolipoproteins: a review. *Eur. Biophys. J.* **31**: 2–8.
26. Hatters, D. M., C. E. MacPhee, L. J. Lawrence, W. H. Sawyer, and G. J. Howlett. 2000. Human apolipoprotein C-II forms twisted amyloid ribbons and closed loops. *Biochemistry.* **39**: 8276–8283.
27. Moore, K. J., J. El Khoury, L. A. Medeiros, K. Terada, C. Geula, A. D. Luster, and M. W. Freeman. 2002. A CD36-initiated signaling cascade mediates inflammatory effects of beta-amyloid. *J. Biol. Chem.* **277**: 47373–47379.
28. Kunjathoor, V. V., A. A. Tseng, L. A. Medeiros, T. Khan, and K. J. Moore. 2004. β -Amyloid promotes accumulation of lipid peroxides by inhibiting CD36-mediated clearance of oxidized lipoproteins. *J. Neuroinflammation.* **1**: article 23.
29. Gordon, D., M. A. Reidy, E. P. Benditt, and S. M. Schwartz. 1990. Cell proliferation in human coronary arteries. *Proc. Natl. Acad. Sci. USA.* **87**: 4600–4604.
30. O'Brien, K. D., K. L. Olin, C. E. Alpers, W. Chiu, M. Ferguson, K. Hudkins, T. N. Wight, and A. Chait. 1998. Comparison of apolipoprotein and proteoglycan deposits in human coronary atherosclerotic plaques: colocalization of biglycan with apolipoproteins. *Circulation.* **98**: 519–527.
31. O'Brien, K. D., D. M. Shavelle, M. T. Caulfield, T. O. McDonald, K. Olin-Lewis, C. M. Otto, and J. L. Probstfield. 2002. Association of angiotensin-converting enzyme with low-density lipoprotein in aortic valvular lesions and in human plasma. *Circulation.* **106**: 2224–2230.
32. O'Brien, K. D., D. Gordon, S. Deeb, M. Ferguson, and A. Chait. 1992. Lipoprotein lipase is synthesized by macrophage-derived foam cells in human coronary atherosclerotic plaques. *J. Clin. Invest.* **89**: 1544–1550.
33. O'Brien, K. D., M. D. Allen, T. O. McDonald, A. Chait, J. M. Harlan, D. Fishbein, J. McCarty, M. Ferguson, K. Hudkins, C. D. Benjamin, et al. 1993. Vascular cell adhesion molecule-1 is expressed in human coronary atherosclerotic plaques. Implications for the mode of progression of advanced coronary atherosclerosis. *J. Clin. Invest.* **92**: 945–951.
34. Pham, C. L., D. M. Hatters, L. J. Lawrence, and G. J. Howlett. 2002. Cross-linking and amyloid formation by N- and C-terminal cysteine derivatives of human apolipoprotein C-II. *Biochemistry.* **41**: 14313–14322.
35. Hatters, D. M., A. P. Minton, and G. J. Howlett. 2002. Macromolecular crowding accelerates amyloid formation by human apolipoprotein C-II. *J. Biol. Chem.* **277**: 7824–7830.
36. Schuck, P. 2000. Size-distribution analysis of macromolecules by sedimentation velocity ultracentrifugation and lamm equation modeling. *Biophys. J.* **78**: 1606–1619.
37. Breathnach, S. M., S. M. Melrose, B. Bhogal, F. C. de Beer, R. F. Dyck, G. Tennent, M. M. Black, and M. B. Pepys. 1981. Amyloid P component is located on elastic fibre microfibrils in normal human tissue. *Nature.* **293**: 652–654.
38. Aquilina, J. A., and C. V. Robinson. 2003. Investigating interactions of the pentraxins serum amyloid P component and C-reactive protein by mass spectrometry. *Biochem. J.* **375**: 323–328.
39. Baltz, M. L., F. C. De Beer, A. Feinstein, and M. B. Pepys. 1982. Calcium-dependent aggregation of human serum amyloid P component. *Biochim. Biophys. Acta.* **701**: 229–236.
40. Mak, P. A., B. A. Laffitte, C. Desrumaux, S. B. Joseph, L. K. Curtiss, D. J. Mangelsdorf, P. Tontonoz, and P. A. Edwards. 2002. Regulated expression of the apolipoprotein E/C-I/C-IV/C-II gene cluster in murine and human macrophages. A critical role for nuclear liver X receptors alpha and beta. *J. Biol. Chem.* **277**: 31900–31908.
41. Steinberg, D., and J. L. Witztum. 2002. Is the oxidative modification hypothesis relevant to human atherosclerosis? Do the antioxidant trials conducted to date refute the hypothesis? *Circulation.* **105**: 2107–2111.
42. Hatters, D. M., N. Zhong, E. Rutenber, and K. H. Weisgraber. 2006. Amino-terminal domain stability mediates apolipoprotein E aggregation into neurotoxic fibrils. *J. Mol. Biol.* **361**: 932–944.
43. Wilson, L. M., C. L. Pham, A. J. Jenkins, J. D. Wade, A. F. Hill, M. A. Perugini, and G. J. Howlett. 2006. High density lipoproteins bind Abeta and apolipoprotein C-II amyloid fibrils. *J. Lipid Res.* **47**: 755–760.
44. Jenny, N. S., A. M. Arnold, L. H. Kuller, R. P. Tracy, and B. M. Psaty. 2007. Serum amyloid P and cardiovascular disease in older men and women. Results from the Cardiovascular Health Study. *Arterioscler. Thromb. Vasc. Biol.* **27**: 352–358.
45. Noursadeghi, M., M. C. Bickerstaff, J. R. Gallimore, J. Herbert, J. Cohen, and M. B. Pepys. 2000. Role of serum amyloid P component in bacterial infection: protection of the host or protection of the pathogen. *Proc. Natl. Acad. Sci. USA.* **97**: 14584–14589.
46. Botto, M., P. N. Hawkins, M. C. Bickerstaff, J. Herbert, A. E. Bygrave, A. McBride, W. L. Hutchinson, G. A. Tennent, M. J. Walport, and M. B. Pepys. 1997. Amyloid deposition is delayed in mice with targeted deletion of the serum amyloid P component gene. *Nat. Med.* **3**: 855–859.
47. Bucciantini, M., E. Giannoni, F. Chiti, F. Baroni, L. Formigli, J. Zurdo, N. Taddei, G. Ramponi, C. M. Dobson, and M. Stefani. 2002. Inherent toxicity of aggregates implies a common mechanism for protein misfolding diseases. *Nature.* **416**: 507–511.